Journal of Luminescence 196 (2018) 285–289

Contents lists available at ScienceDirect

Journal of Luminescence

journal homepage: www.elsevier.com/locate/jlumin

Effect of ionic substitution (Ca/Sr/Ba) on structure and luminescent properties of Ce^{3+} doped fluorapatite

Qingfeng Guo[a,*], Libing Liao[b,*], Stefan Lis[c], Haikun Liu[b], Lefu Mei[b,*]

[a] School of Gemology, China University of Geosciences, Jewelry and Mineral Materials Laboratory of Experimental Teaching Demonstration Center, Beijing 100083, China
[b] Beijing Key Laboratory of Materials Utilization of Nonmetallic Minerals and Solid Wastes, National Laboratory of Mineral Materials. School of Materials Sciences and Technology, China University of Geosciences, Beijing 100083, China
[c] Adam Mickiewicz University, Faculty of Chemistry, Department of Rare Earths, Umultowska 89b, 61-614 Poznań, Poland

ARTICLE INFO

Keywords:
Fluorapatite
Phosphor
Photoluminescence
Red-shift
Iso-structural

ABSTRACT

In this paper, Ce^{3+}-activated iso-structural solid solutions $La_{5.99}Ce_{0.01}M_4(SiO_4)_6F_2$ (M = Ca, Sr and Ba) compounds were prepared for the first time. The structure and luminescence properties of the samples were investigated to explore the difference of cation substitution. The phase analysis indicated that all XRD peaks of the samples were indexed by a hexagonal cell with the space group of $P6_3/m$, and the phosphors showed strong blue light emission with broad bands. With the isomorphous substitution of Ba → Sr → Ca, the average bond length between Ce^{3+} and anions is decreased and the crystal field around Ce^{3+} is strengthened, resulting in the red-shift (from 410 nm to 423 nm) of the emission wavelength for $La_{5.99}Ce_{0.01}M_4(SiO_4)_6F_2$ (M = Ca, Sr, Ba).

1. Introduction

As the next generation light source, white-light-emitting diodes (*w*-LEDs) has many advantages such as long lifetime, environmental friendliness, high efficiency [1,2]. Accordingly, to be an important part of *w*-LEDs, novel phosphors have received a lot of attentions with the development of *w*-LEDs [3–5]. As we know, lanthanide ions play an important and irreplaceable role in phosphors due to their 5*d* → 4*f* or 4*f* → 4*f* transitions [6–10]. Among lanthanide ions, Ce^{3+} has been considered as an ideal activator with a broad band covering blue color to red color because the outermost 5*d* electron of Ce^{3+} is sensitive to the crystal field [11,12].

wOn the other hand, based on their excellent chemical and thermal properties, apatite compounds with the general chemical formula of $A_5(BO_4)_6C$ (A = Ca^{2+}, Sr^{2+}, Ba^{2+}, Eu^{2+}, La^{3+},etc.; B = P^{5+}, As^{5+}, Si^{4+}, S^{6+}, etc.; C = F^-, Cl^-, OH^-, etc.) were used as effective host materials for phosphors, such as $KLaSr_3(PO_4)_3F:Eu^{2+}$ [13], $Ca_4Y_6(SiO_4)_6O:Ce^{3+}/Mn^{2+}/Tb^{3+}$ [14], and $La_5Si_2BO_{13}$: Ce^{3+}, Mn^{2+} [15]. Apatite contains two different cation sites: the seven-fold coordinated 6*h* sites with a C_S point symmetry and the nine-fold coordinated 4*f* sites with C_3 point symmetry. Both sites are suitable and easy for the substitution of lanthanide ions. As discussed above, the 5d electron of Ce^{3+} is sensitive to the crystal field. Therefore, it is interesting to obtain color-tunable Ce^{3+} emission by doping Ce^{3+} into a series of apatite solid solution hosts.

In our previous work, a series of blue-emitting $La_{5.90-x}Ba_{4+x}(SiO_4)_{6-x}(PO_4)_xF_2$: $0.10Ce^{3+}$ (x = 0, 1, 2, and 3) phosphors with apatite structure were synthesized by a solid-state reaction. The phosphor showed excellent luminescent properties [16]. By isomorphous substitution of cations (Ca^{2+} = Sr^{2+} = Ba^{2+}), we expect some interesting luminescence behaviors in apatite structure $La_{5.99}Ce_{0.01}M_4(SiO_4)_6F_2$ (M = Ca, Sr, Ba).

In this paper, the solid solutions of $La_{5.99}Ce_{0.01}M_4(SiO_4)_6F_2$ (M = Ca, Sr, Ba) were synthesized successfully and the crystal environment variation of Ce^{3+} has been realized by isomorphous substitution of cation (Ca^{2+} = Sr^{2+} = Ba^{2+}). The emission band shows a red-shift (from 410 nm to 423 nm) for $La_{5.99}Ce_{0.01}M_4(SiO_4)_6F_2$ (M = Ca, Sr, Ba) with the isomorphous substitute for Ba → Sr → Ca. By analyzing the crystal structure and changes of luminescence, the relationship between the crystal structure evolution and luminescence property was discussed.

2. Experimental

2.1. Synthesis procedures

$La_{5.99}Ce_{0.01}M_4(SiO_4)_6F_2$ (M = Ca, Sr, Ba) samples were prepared by a traditional high temperature solid-state reaction. The raw materials were $CaCO_3$ (Aldrich, 99.9%), $SrCO_3$ (Aldrich, 99.9%), $BaCO_3$ (Aldrich, 99.9%), SiO_2 (Aldrich, 99.9%), La_2O_3 (Aldrich, 99.995%), and CeO_2

* Corresponding authors.
E-mail addresses: qfguo@cugb.edu.cn (Q. Guo), clayl@cugb.edu.cn (L. Liao), mlf@cugb.edu.cn (L. Mei).

https://doi.org/10.1016/j.jlumin.2017.12.051
Received 30 October 2017; Received in revised form 18 December 2017; Accepted 24 December 2017
Available online 25 December 2017

(Aldrich, 99.995%). After they were weighed and thoroughly mixed by grinding in an agate mortar, the mixtures were placed into corundum crucibles, preheated at 750 °C for 3 h in alumina crucibles in a muff furnace in the air. After that, the samples were ground thoroughly and sintered at 1400 °C for 4 h in a reducing atmosphere with flowing gas (10% H_2 + 90% N_2), then slowly cooled to room temperature naturally. Finally, the samples were ground again into powder for measurements.

2.2. Characterization

The crystal structures of the synthesized samples were examined by using a X-ray powder diffractometer (XRD; D8 Advance diffractometer, Germany) with Cu Kα radiation (λ = 1.5418 Å) from 10° to 60° (2θ). The photoluminescence (PL) and photoluminescence excitation (PLE) spectra of the samples were measured by using an F-4600 fluorescence spectrophotometer equipped with a 150 W Xe light. All of the measurements were performed at room temperature.

3. Results and discussion

3.1. Phase identification and structure analysis

Fig. 1 shows the crystal structure of $La_{5.99}Ce_{0.01}M_4(SiO_4)_6F_2$ (M = Ca, Sr, Ba) samples along the *c* axis. As shown in Fig. 1, two cationic sites exist in the structure: 9-fold coordinated 4f sites with C_3 point symmetry and 7-fold coordinated 6 h sites with C_s point symmetry. To verify the phase purity and structure, all samples were characterized by XRD. Fig. 2(a) shows the XRD patterns of $La_{5.99}Ce_{0.01}M_4(SiO_4)_6F_2$ (M = Ca, Sr, Ba) samples, and the calculated standard profile of $La_6Ba_4(SiO_4)_6F_2$ (ICSD no. 170852) is shown as a reference. It is obvious that all the XRD patterns are consistent with that of the standard $La_6Ba_4(SiO_4)_6F_2$ [17], which indicates that $La_{5.99}Ce_{0.01}M_4(SiO_4)_6F_2$ (M = Ca, Sr, Ba) samples are isostructural with $La_6Ba_4(SiO_4)_6F_2$ and the substitution of Ca^{2+}, Sr^{2+} and Eu^{2+} do not cause any significant impurities. In addition, the XRD patterns of $La_{5.99}Ce_{0.01}M_4(SiO_4)_6F_2$ (M = Ca, Sr and Ba) samples fitted by Gaussian functions with 2θ ranging from 30° to 31.5° is shown in Fig. 2(b). As depicted in Fig. 2(b), all the XRD peaks located at about 30.5° for all the samples can be well fitted by two gaussian peaks, attributed to the diffractions of (121) and (112) lattice plane. The diffractions of (121) and (112) lattice plane for $La_{5.99}Ce_{0.01}M_4(SiO_4)_6F_2$ (M = Ca, Sr and Ba) samples are illustrated in Fig. 2(d). With the isomorphous substitute for Ba^{2+}→Sr^{2+}→Ca^{2+}, both the diffraction peaks of (121) and (112) crystal face shifted slightly to the larger angle side, which can be ascribed to the substitution of Ba^{2+} by smaller Sr^{2+} and Ca^{2+}. The cell parameters of $La_{5.99}Ce_{0.01}M_4(SiO_4)_6F_2$ (M = Ca, Sr and Ba) samples are shown in Fig. 2(c) and Table 1. It can be seen that the cell parameters for the samples decreased with the isomorphous substitute for Ba^{2+} → Sr^{2+} → Ca^{2+}. The bond lengths (nm) of $La_{5.99}Ce_{0.01}M_4(SiO_4)_6F_2$ (M = Ca, Sr and Ba) crystal lattice obtained from the X-ray powder diffraction data is shown in Table 2 and Fig. 3, which will be discussed in the part of photoluminescence properties.

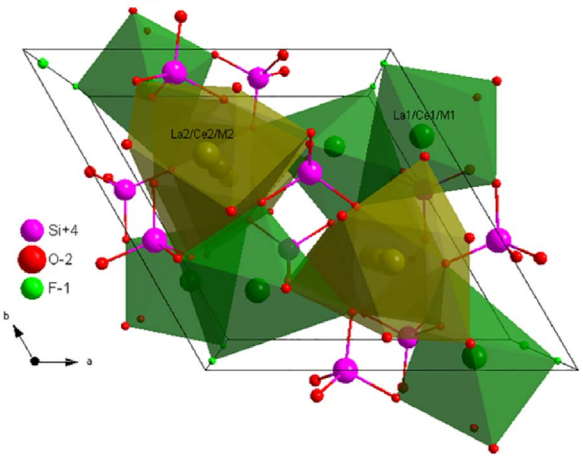

Fig. 1. The crystal structure of $La_{5.99}Ce_{0.01}M_4(SiO_4)_6F_2$ (M = Ca, Sr, Ba) samples view the *c* axis.

3.2. Photoluminescence properties

Various chemical compositions will produce different crystal field environment for Ce^{3+} ions in solid solution compounds $La_{5.99}Ce_{0.01}M_4(SiO_4)_6F_2$ (M = Ca, Sr and Ba), affecting the luminescence properties of the as-prepared solid solution phosphors. The normalized PLE and PL spectra of $La_{5.99}Ce_{0.01}M_4(SiO_4)_6F_2$ (M = Ca, Sr and Ba) samples are illustrated in Fig. 4. All the PLE spectra of the sample exhibit strong broad absorption bands in the range of 230–380 nm ascribed to the 4*f*–5*d* transition of Ce^{3+} [18,19], indicating all the phosphors can be efficiently excited by UV and *n*-UV light. However, the PL spectra of $La_{5.99}Ce_{0.01}M_4(SiO_4)_6F_2$ (M = Ca, Sr and Ba) show a red-shift from 410 nm to 423 nm with the isomorphous substitute for Ba → Sr → Ca. As is known to us, the local environment of the Ce^{3+} sites are significantly changed attributed to the changes in bond-length between Ce^{3+} and the surrounding ligand anion, which can be determined by the following equation [20,21]:

$$D_q = \frac{ze^2r^4}{6R^5} \tag{1}$$

in which D_q stands for the energy level separation, *z* is the charge or valence of the anion ligand, *e* represents the charge of an electron, *r* is the radius of the *d* wave function, and *R* is the distance between the central ion and its ligands. It is clear that the *z*, *e* and *r* values are the same in $La_{5.99}Ce_{0.01}M_4(SiO_4)_6F_2$ (M = Ca, Sr and Ba) phosphors, indicating that *Dq* is only the function of $1/R^5$. Therefore, if *R* is the smaller, D_q has the larger value, which results in the red-shift of the emission peak. In our case, *R* is the distance between Ce^{3+} and F^-/O^{2+}. As illustrated in Table 2, Both the average *R* values for Ce1-F/O and Ce2-F/O decrease with the substitute for Ba → Sr → Ca. Therefore, the crystal field splits easily resulting in the red-shift of the emission wavelength.

As mentioned above, two Ce^{3+} luminescent centers exist in the crystal lattice of $La_{5.99}Ce_{0.01}M_4(SiO_4)_6F_2$ (M = Ca, Sr and Ba) samples. All the shape of PL spectra (Fig. 5) for the phosphors is asymmetric, and each PL band could be well fitted by a sum of two Gaussian bands consistent with the afore mentioned crystallographic occupancy of Ce^{3+} sites, as depicted in Fig. 5. The emission peaks of two different kinds of Ce^{3+} are marked as Ce1 and Ce2. According to the report of Van Uitert, the energy (E) of the lower *d*-band edge for Ce^{3+} can be represented by the following equation: [22,23]

$$E = Q\left[1 - \left(\frac{V}{4}\right)^{\frac{1}{V}} 10^{-\frac{n \times Ea \times r}{80}}\right] \tag{2}$$

where *E* stands for the position of the rare-earth ion (Ce^{3+} in this paper) emission peak (cm^{-1}), *Q* is the energy position of the lower *d*-band edge for the free ion, *V* represents the valence of the activator Ce^{3+} ion (*V* = 3), *n* is the number of anions in the immediate shell around the Ce^{3+} ion, and *r* is the radius of the host cation replaced by the Ce^{3+} ion (in Å), and *Ea* is the electron affinity of the atoms that form anions (eV). In general, *Ea* is constant in the same host, it is sure that all the structure of $La_{5.99}Ce_{0.01}M_4(SiO_4)_6F_2$ (M = Ca, Sr and Ba) samples are close to the standard $La_6Ba_4(SiO_4)_6F_2$ (ICSD no. 170852). Under the circumstances, the position of the Ce^{3+} emission peak is proportional to the product of *n* and *r*. As shown in Table 2, both the values of *r* and *n* for Ce1 is bigger than that of Ce2 in all the three samples. Therefore, the band peaked at short-wavelength (with higher energy) is attribute to